DOI: 10.1002/zaac.200800167

Organometallic Compounds of the Lanthanides. 183 [1]

Lanthanide Benzyl Complexes of the Type $[Li(tmeda)_2][Ln(CHRSiMe_2R')_3Cl]$ (Ln = Pr, Nd, Sm, Er, Lu; R = Ph, 3,5-$Me_2C_6H_3$; R′ = Me, ^{t}Bu, Ph) and $[Li(tmeda)]_2(\mu\text{-}Cl)_3Ln(CHPhSiMe_2{}^tBu)_2$ (Ln = Er, Lu)

Herbert Schumann*, Dominique M. M. Freckmann, and Sebastian Dechert

Berlin, Institut für Chemie der Technischen Universität

Received April 26th, 2008.

Dedicated to Professor Bernt Krebs on the Occasion of his 70th Birthday

Abstract. $PrCl_3$, $NdCl_3$, $SmCl_3$, $ErCl_3$, and $LuCl_3$ react with three mole equivalents of [Li(tmeda)][$CHPhSiMe_3$] (**1**), [Li(tmeda)][$CHPhSiMe_2{}^tBu$] (**2**), [Li(tmeda)][$CHPhSiMe_2Ph$] (**3**), and [Li(tmeda)][$CH(C_6H_3Me_2$-3,5)$SiMe_2{}^tBu$] (**4**) forming the *ate* complexes $[Li(tmeda)_2][Ln(CHPhSiMe_3)_3Cl]$ (Ln = Pr (**5a**), Nd (**6a**), Sm (**7a**)), $[Li(tmeda)_2][Ln(CHPhSiMe_2{}^tBu)_3Cl]$ (Ln = Pr (**5b**), Nd (**6b**), Sm (**7b**)), $[Li(tmeda)_2][Pr(CHPhSiMe_2Ph)_3Cl]$ (**5c**), and $[Li(tmeda)_2][Ln(CH(C_6H_3Me_2$-3,5)$SiMe_2{}^tBu)_3Cl]$ (Ln = Er (**8d**), Lu (**9d**)). $\{[Li(tmeda)]_2[Nd(CHPhSiMe_3)Cl_4]\}_2$ (**10**) and $\{[Li(tmeda)][Nd(CHPhSiMe_3)Cl_3(THF)]\}_2$ (**11**) crystallize from concentrated ethereal solutions of **6a** after addition of pentane. **4** reacts with two equivalents of $ErCl_3$ and $LuCl_3$ yielding $[Li(tmeda)]_2(\mu\text{-}Cl)_3Ln(CHPhSiMe_2{}^tBu)_2$ (Ln = Er (**12**), Lu (**13**)). Compounds **7a**,**b**, **9d**, and **13** have been characterized by ^1H and **9d** and **13** also by ^{13}C NMR spectroscopy, compounds **6b**, **7a**, **8d**, **9d**, **10**, **11**, **12**, and **13** by X-ray structure analysis.

Keywords: Praseodymium; Neodymium; Samarium; Erbium; Lutetium; Benzyl complexes; NMR; Crystal structure

Introduction

The chemistry of alkyl lanthanide compounds is still a quite disregarded area of the f-element chemistry. Only some of the few known organo lanthanide compounds containing exclusively σ-bonded alkyl ligands have been characterized structurally [2]. Within this field of research, homoleptic benzyl lanthanide complexes are of special interest because of their promising usability as starting materials for the preparation of highly active polymerization catalysts. After the isolation of $Sc(CH_2C_6H_4NMe_2)_3$ by *Manzer* in 1978 [3] and the following attempts of Russian research groups [4] and of *Thiele* et al. [5] to synthesize benzyl lanthanides, in 1997 *Magull* et al. published the first X-ray structure of the rare earth benzyl complex $[(tmeda)(PhCH_2)_2Y(\mu\text{-}Br)_2Li(tmeda)]$, a complex having no cyclopentadienyl or alike ligands additionally bonded to the central metal [6]. Very recently, the solvent free homoleptic benzyl complexes $Ln(CH_2C_6H_4NMe_2)_3$ (Ln = Y, La) [7], the THF stabilized complexes $La(CH_2Ph)_3(THF)_3$, $La(CH_2C_6H_4Me)_3(THF)_3$ [8] and $Sc(CH_2Ph)_3(THF)_2$ [9], as well as $Ln(CH_2C_6H_4NMe_2$-2)$_3Ln$, $Ln(CH_2Ph)_3(THF)_3$, $Ln(CH_2C_6H_4{}^tBu$-4)$_3(THF)_3$, and $Eu[CH(SiMe_3)C_6H_4NMe_2$-2]$_2(THF)_2$ [10] have been described as extraordinarily stable compounds. They have been characterized by X-ray structure analyses and were partly used as catalysts in ethylene polymerization and hydroamination reactions [8].

In the course of our efforts to synthesize solvent free benzyl complexes of the lanthanides which are not stabilized by chelation of heteroatoms containing substituents at the benzyl ligands like -OMe or -NMe_2 groups, but by sterically demanding groups, we first investigated the benzhydryl anion $CHPh_2^-$ [11]. The results of our following studies concerning the use of benzyl ligands containing triorganosilyl groups bonded to the benzyl C_α-carbon atom are presented here.

Results and Discussion

Synthesis of $[Li(tmeda)_2][Ln(CHRSiMe_2R')_3Cl]$

$PrCl_3$, $NdCl_3$, $SmCl_3$, $ErCl_3$, and $LuCl_3$ or their THF adducts $LnCl_3(THF)_n$ react with three mole equivalents of [Li(tmeda)][$CHPhSiMe_3$] (**1**) [12], [Li(tmeda)][$CHPhSiMe_2{}^tBu$] (**2**) [13], [Li(tmeda)][$CHPhSiMe_2Ph$] (**3**) [13], and [Li(tmeda)][$CH(C_6H_3Me_2$-3,5)$SiMe_2{}^tBu$] (**4**) [13] in THF at ambient temperature forming the *ate* complexes $[Li(tmeda)_2][Ln(CHPhSiMe_3)_3Cl]$ (Ln = Pr (**5a**), Nd (**6a**),

* Prof. Dr. H. Schumann
Institut für Chemie,
Sekr. C2 der Technischen Universität
Straße des 17. Juni 135
D-10623 Berlin
Fax: +49-(0)30-31422168
E-mail: Schumann@chem.tu-berlin.de

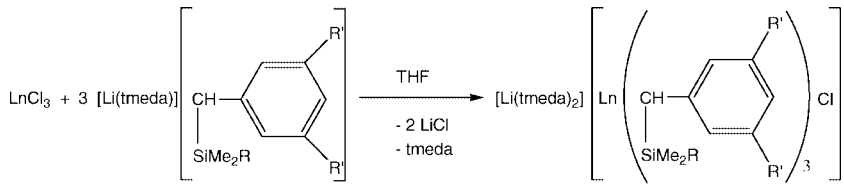

1, **2**, **3**, **4**

Ln/ R/R'	Me/H	^{t}Bu/H	Ph/H	^{t}Bu/Me
Pr	**5a**	**5b**	**5c**	
Nd	**6a**	**6b**		
Sm	**7a**	**7b**		
Er				**8d**
Lu				**9d**

Scheme 1

Sm (**7a**)), [Li(tmeda)$_2$][Ln(CHPhSiMe$_2$^{t}Bu)$_3$Cl] (Ln = Pr (**5b**), Nd (**6b**), Sm (**7b**)), [Li(tmeda)$_2$][Pr(CHPhSiMe$_2$Ph)$_3$Cl] (**5c**), and [Li(tmeda)$_2$][Ln(CH(C$_6$H$_3$Me$_2$-3,5)SiMe$_2$^{t}Bu)$_3$Cl] (Ln = Er (**8d**), Lu (**9d**)) (Scheme 1).

The immediate change in color of the reaction mixtures during the addition of the respective lithium benzylate to pale green (**5a**,**b**,**c**), orange-green (**6a**,**b**), purple (**7a**,**b**), pink (**8d**), and light yellow (**9d**) indicates a straight course of the reactions. The oily substances remaining after removal of the solvent were extracted with diethyl ether and the extracts were filtered off from precipitated lithium chloride. Cooling of the concentrated ethereal extracts to −36 °C or covering these solutions with a layer of pentane at room temperature afforded the crystalline products. The oxygen and water sensitive compounds decompose above 100 °C and can be stored under nitrogen at room temperature for several weeks.

The ^{1}H NMR spectra of the samarium complexes **7a** and **7b** and the lutetium compound **9d** as well as the ^{13}C NMR spectrum of **9d** show the expected signals.

In the case of compounds **6b**, **7a**, **8d**, and **9d** we succeeded in the isolation of single crystals suitable for X-ray structural analysis. The attempt to get single crystals of **6a** by layering its concentrated ethereal solution with pentane at room temperature surprisingly caused the precipitation of green and orange crystals. The X-ray structural analysis of single crystals picked out of the respective crop, proved the green crystals to be {[Li(tmeda)]$_2$[Nd(CHPhSiMe$_3$)Cl$_4$]}$_2$ (**10**) and the orange crystals to be {[Li(tmeda)]-[Nd(CHPhSiMe$_3$)Cl$_3$(THF)]}$_2$ (**11**).

Solid State Structures of 6b, 7a, 8d, 9d, 10, *and* 11

The molecular structures of **6b**, **7a**, **8d**, **9d**, **10**, and **11** were determined by single crystal X-ray diffraction analysis. Complex **9d** crystallizes isotypically with **8d**. The molecular structure of the anions of **6b**, **7a**, and **8d** are depicted in Figures 1 to 3, respectively. One tmeda molecule in **7a** is disordered between two positions. **8d** as well as **9d** comprises two molecules of Et$_2$O per formula unit. In both cases, one Et$_2$O molecule is disordered between two positions.

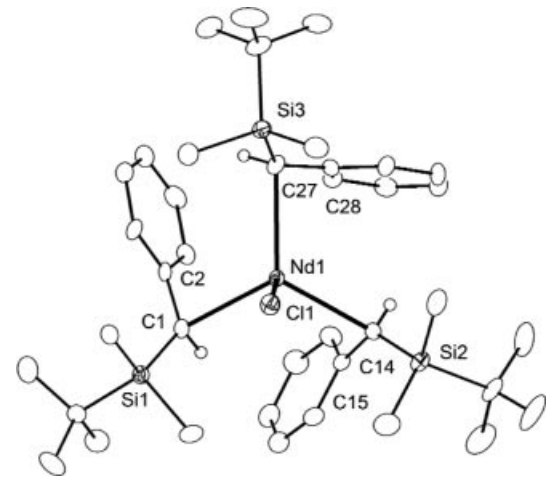

Fig. 1 Molecular structure of the anionic part of **6b**. The hydrogen atoms except the benzyl C$_\alpha$ protons are omitted for clarity. Thermal ellipsoids are drawn with 30 % probability.

Selected bond lengths / Å and angles / °: Nd(1)-Cl(1) 2.6489(16), Nd(1)-C(1) 2.567(6), Nd(1)-C(2) 2.864(5), Nd(1)-C(14) 2.558(6), Nd(1)-C(15) 2.848(6), Nd(1)-C(27) 2.597(7), Nd(1)-C(28) 2.845(6), Si(1)-C(1) 1.840(6), Si(2)-C(14) 1.843(7), Si(3)-C(27) 1.841(7), C(1)-C(2) 1.461(8), C(14)-C(15) 1.447(9), C(27)-C(28) 1.454(8); Nd(1)-C(1)-C(2) 86.0(3), Nd(1)-C(14)-C(15) 85.9(4), Nd(1)-C(27)-C(28) 84.2(4), C(1)-Nd(1)-Cl(1) 97.36(15), C(2)-Nd(1)-Cl(1) 113.32(13), C(14)-Nd(1)-Cl(1) 96.53(15), C(15)-Nd(1)-Cl(1) 112.85(13), C(27)-Nd(1)-Cl(1) 97.45(15), C(28)-Nd(1)-Cl(1) 112.77(13), C(1)-Nd(1)-C(14) 117.9(2), C(1)-Nd(1)-C(27) 117.8(2), C(14)-Nd(1)-C(27) 119.7(2), C(1)-Nd(1)-C(2) 30.58(18), C(14)-Nd(1)-C(15) 30.45(18), C(27)-Nd(1)-C(28) 30.56(18), Si(1)-C(1)-Nd(1) 120.2(3), Si(2)-C(14)-Nd(1) 123.5(3), Si(3)-C(27)-Nd(1) 121.8(3).

The molecular structures prove the *ate*-character of the compounds showing separated cations and anions. The lithium cations are coordinated by two tmeda molecules. The anions consist of the respective lanthanide atom placed in the center of a distorted tetrahedron formed by three benzyl ligands and one chlorine atom. Analogous tetrahedral ligand arrangements around a central lanthanide atom are found in [Li(THF)$_4$][Yb{CH(SiMe$_3$)$_2$}$_3$Cl] [14] as well as in the coordination polyhedrons of Nd(OC^{t}Bu$_3$)$_3$(μ-Cl)Li(THF)$_3$ [15], Nd[N(SiMe$_3$)$_2$]$_3$(μ-Cl)Li(THF)$_3$ [15], Ln[CH(SiMe$_3$)$_2$]$_3$(μ-Cl)Li(L)$_x$ (Ln = La, L = pmdta, x = 1; Ln = Y, L = Et$_2$O, x = 3) [16], Sm[CH(SiMe$_3$)$_2$]$_3$(μ-

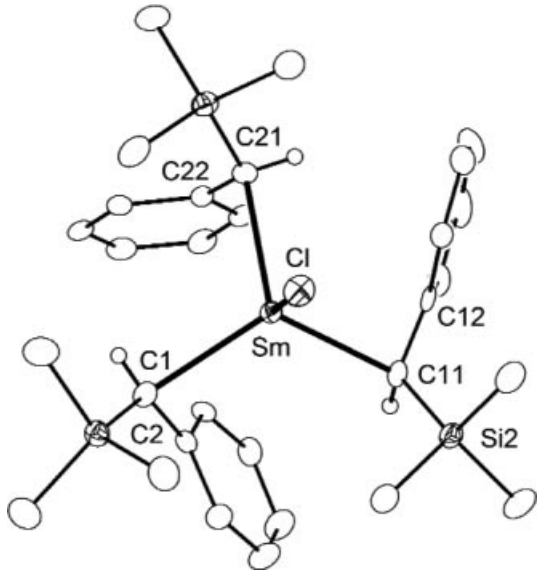

Fig. 2 Molecular structure of the anionic part of **7a**. The hydrogen atoms except the benzyl C_α protons are omitted for clarity. Thermal ellipsoids are drawn with 30 % probability.

Selected bond lengths / Å and angles / °: Sm-Cl 2.6063(15), Sm-C(1) 2.564(6), Sm-C(2) 2.787(5), Sm-C(11) 2.483(5), Sm-C(12) 2.906(5), Sm-C(21) 2.533(5), Sm-C(22) 3.041(5), Si(1)-C(1) 1.825(6), Si(2)-C(11) 1.844(6), Si(3)-C(21) 1.844(6), C(1)-C(2) 1.466(7), C(11)-C(12) 1.463(8), C(21)-C(22) 1.463(7); Sm-C(1)-C(2) 82.7(3), Sm-C(11)-C(12) 91.1(3), Sm-C(21)-C(22) 95.4(3), C(1)-Sm-Cl 100.89(13), C(2)-Sm-Cl 121.23(12), C(11)-Sm-Cl 98.75(13), C(12)-Sm-Cl 100.93(10), C(21)-Sm-Cl 101.98(13), C(22)-Sm-Cl 128.34(10), C(1)-Sm-C(11) 120.27(17), C(1)-Sm-C(21) 123.16(15), C(11)-Sm-C(21) 117.92(19), C(1)-Sm-C(2) 31.45(15), C(11)-Sm-C(12) 30.21(16), C(21)-Sm-C(22) 28.61(15), Si(1)-C(1)-Sm 127.6(3), Si(2)-C(11)-Sm 120.0(3), Si(3)-C(21)-Sm 116.5(3).

Me)Li(pmdta) [17], and $Ln[N(SiMe_2CH_2CH_2SiMe_2)]_3(\mu\text{-}Cl)Li(THF/Et_2O)_3$ [18] in which either a methyl group or a chlorine atom functions as bridge between the lanthanide and the solvated lithium atom.

Though the molecular structures described here do not show a chlorine bridge between the lanthanide atom and the coordinatively satisfied lithium atom, it is to note, that in **6b**, **8d**, and **9d** the alignment of the Ln-Cl bond to the lithium atom of a neighboring cation is almost linear (Ln-Cl···Li (°) / Cl···Li (Å): 174 / 4.69 for **6b**, 179 / 4.61 for **8d**, 179 / 4.56 for **9d**), whereas the Sm-Cl bond axis in **7a** does not point in the direction of any neighboring lithium cation (Cl-Sm···Li = 103°).

The Ln-Cl distances (2.65 (**6b**), 2.61 (**7a**), 2.53 (**8d**), 2.49 (**9d**) Å) lie in the range of the Ln-Cl bond lengths of other lanthanide complexes containing one terminal chlorine atom e.g. $NdCl[N(C_6H_3{}^iPr_2)(SiMe_3)]_2(THF)$ (2.62 Å) [19], $SmCl[Me_2Si(C_5H_2{}^tBuMe)(C_5H_3C_2H_4NMe_2)]$ (2.64 Å) [20], $ErCl(C_5H_4CH_2Ph)_2(THF)$ (2.54 Å) [21], and $LuCl(C_5H_2{}^tBuMe\text{-}SiMe_2\text{-}C_9H_5C_2H_4NMe_2)$ (2.49 Å) [22]. The lanthanide contraction accounting for the differences in the effective ionic radii of the Ln^{3+} ions [23] becomes apparent in the decrease of the Ln-Cl distances in the series **6b** > **7a** > **8d** > **9d**.

The comparison of the distances and angles between the respective central lanthanide atom and the C_α and C_{ipso} carbon atoms of the three benzyl ligands allows some interesting conclusions with respect to the type of bonding (Table 1).

In **6b**, the Nd atom is situated above the phenyl planes of all three benzyl ligands in an almost symmetrical fashion. Since the benzyl C_α atoms are slightly turned out from the respective phenyl plane towards the neodymium atom, the Nd-C_α bond axes do not run perpendicular to these planes,

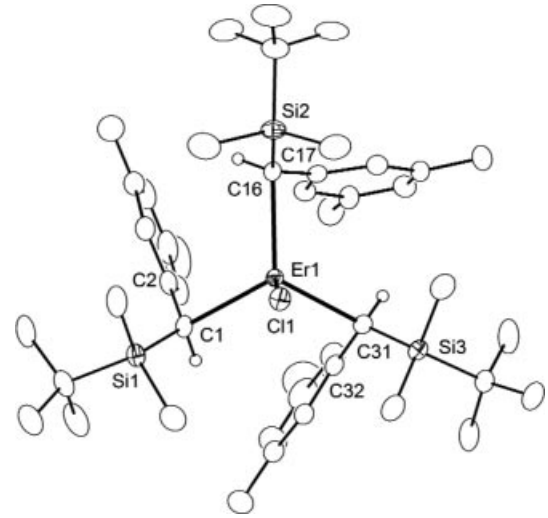

Fig. 3 Molecular structure of the anionic part of **8d**. The hydrogen atoms except the benzyl C_α protons are omitted for clarity. Thermal ellipsoids are drawn with 30 % probability.
Selected bond lengths / Å and angles / ° for **8d** and the isotypic anion of **9d**.

8d: Er(1)-Cl(1) 2.5271(13), Er(1)-C(1) 2.457(4), Er(1)-C(2) 2.919(5), Er(1)-C(16) 2.465(5), Er(1)-C(17) 2.713(5), Er(1)-C(31) 2.417(5), Er(1)-C(32) 2.948(5), Si(1)-C(1) 1.842(5), Si(2)-C(16) 1.830(5), Si(3)-C(31) 1.852(5), C(1)-C(2) 1.457(7), C(16)-C(17) 1.447(6), C(31)-C(32) 1.471(7); Er(1)-C(1)-C(2) 92.9(3), Er(1)-C(16)-C(17) 83.5(3), Er(1)-C(31)-C(32) 95.5(3), C(1)-Er(1)-Cl(1) 100.38(12), C(2)-Er(1)-Cl(1) 123.67(10), C(16)-Er(1)-Cl(1) 96.56(11), C(17)-Er(1)-Cl(1) 116.47(11), C(31)-Er(1)-Cl(1) 99.61(12), C(32)-Er(1)-Cl(1) 112.89(12), C(1)-Er(1)-C(16) 117.33(17), C(1)-Er(1)-C(31) 116.55(17), C(16)-Er(1)-C(31) 119.17(16), C(1)-Er(1)-C(2) 29.91(16), C(16)-Er(1)-C(17) 31.99(14), C(31)-Er(1)-C(32) 29.78(14), Si(1)-C(1)-Er(1) 121.1(2), Si(2)-C(16)-Er(1) 126.6(2), Si(3)-C(31)-Er(1) 121.8(2).

9d: Lu(1)-Cl(1) 2.488(3), Lu(1)-C(1) 2.392(10), Lu(1)-C(2) 2.969(13), Lu(1)-C(16) 2.425(11), Lu(1)-C(17) 2.732(12), Lu(1)-C(31) 2.379(11), Lu(1)-C(32) 2.987(13), Si(1)-C(1) 1.838(13), Si(2)-C(16) 1.838(11), Si(3)-C(31) 1.846(12), C(1)-C(2) 1.49(2), C(16)-C(17) 1.489(16), C(31)-C(32) 1.468(17); Lu(1)-C(1)-C(2) 97.2(8), Lu(1)-C(16)-C(17) 84.9(7), Lu(1)-C(31)-C(32) 99.2(7), C(1)-Lu(1)-Cl(1) 102.2(3), C(2)-Lu(1)-Cl(1) 125.5(2), C(16)-Lu(1)-Cl(1) 99.4(3), C(17)-Lu(1)-Cl(1) 119.7(3), C(31)-Lu(1)-Cl(1) 101.6(3), C(32)-Lu(1)-Cl(1) 113.6(3), C(1)-Lu(1)-C(16) 115.0(5), C(1)-Lu(1)-C(31) 113.3(5), C(16)-Lu(1)-C(31) 120.9(4), C(1)-Lu(1)-C(2) 29.8(5), C(16)-Lu(1)-C(17) 32.9(4), C(31)-Lu(1)-C(32) 29.0(4), Si(1)-C(1)-Lu(1) 121.6(6), Si(2)-C(16)-Lu(1) 124.7(5), Si(3)-C(31)-Lu(1) 121.1(6).

Table 1 Selected bond lengths / Å and angles / ° for **6b**, **7a**, **8d**, and **9d**.

	Ln-C_α	Ln-C_i	Δ(Ln-C_i / Ln-C_α)	∠(Ln-C_α-C_i)
6b (Nd)	2.56−2.60	2.85−2.86	~ 10 %	84.2−86.0
7a (Sm)	2.48−2.56	2.79; 2.91; 3.04	10−20 %	82.7; 91.1; 95.4
8d (Er)	2.42−2.47	2.71; 2.92; 2.95	10−20 %	83.5; 92.9; 95.5
9d (Lu)	2.39−2.43	2.73; 2.97; 2.99	10−20 %	84.9; 97.2; 99.2

but are somewhat bent towards the respective C_α proton. The Nd-C_α and Nd-C_i distances as well as the Nd-C_α-C_i angles are almost equal among each other with the Nd-C_i distances being longer than the Nd-C_α distances by 10 % and the three Nd-C_α-C_i angles being smaller than 90°. In **7a**, the differences between the corresponding distances, distance ratios, and angles are more pronounced. The distances of the samarium atom to the C_i atoms of the three benzyl ligands differ by 0.1 Å each time with the shortest distance showing a value below the shortest Nd-C_i distances in **6b**. At the same time, the angles Sm-C_α-C_i increase stepwise. Two of the C_α atoms are slightly turned out from the appropriate phenyl plane, whereas the third benzyl ligand is approximately planar. Thus, the axes of two Sm-C_α bonds do not run perpendicular to the respective phenyl plane, but are bent, one towards the C_α proton, the other towards the silicon atom of the respective benzyl ligand.

In the complexes **8d** and **9d** with the smaller lanthanides Er and Lu two of the three benzyl ligands show slightly shorter Ln-C_α distances, considerable longer Ln-C_i distances and larger Ln-C_α-C_i angles than the third one. The benzyl moieties are also slightly bent and all Ln-C_α bond axes deviate considerably from a perpendicular alignment towards the phenyl ring planes. In **8d** the three axes incline towards the respective silicon atoms while in **9d** two axes incline towards the C_α-hydrogen atom while the third axis inclines towards the silicon atom of the respective benzyl ligand.

The primary bonding interactions between the lanthanide atoms and the benzyl ligands occur by the Ln-C_α bonds. The average bond lengths Nd-C_α = 2.58 Å, Sm-C_α = 2.53 Å, Er-C_α = 2.47 Å, and Lu-C_α = 2.40 Å are only slightly longer than the Ln-C bonds in the complexes $Ln(CH_2SiMe_3)_3(THF)_{2/3}$ (Ln = Sm: 2.49 Å, Er: 2.41 Å, Lu: 2.36 Å) [24] and fit well in the series of previously reported Ln-CH_2Ph distances of 2.60 Å for $(C_5Me_5)_2CeCH_2Ph$ [25], 2.53 Å for $C_5Me_5Gd(CH_2Ph)_2(THF)$ [26], and 2.55 and 2.56 Å for $[(C_5Me_5)_2Sm(CH_2Ph)_2K(THF)_2]_n$ [26].

The Ln-C_α-C_i angles in **6b**, **7a**, **8d**, and **9d** are significantly smaller than it would be expected for η^1-bonded benzyl ligands since in η^1-bonded benzyl yttrium and samarium complexes the values of the M-C_α-C_i angles range between 109 and 130° [6, 26–28]. However, M-C_α-C_i angels of about 90° have been measured for polar benzyl complexes of lithium [13], early transition metals like zirconium [29], cerium (86.0° in $(C_5Me_5)_2CeCH_2Ph$)) [25], gadolinium (92.1° and 96.4° in $C_5Me_5Gd(CH_2Ph)_2(THF)$) [26], and some actinides [30, 31]. They were interpreted in the sense of η^2-bonding benzyl systems according to interactions between the metal and the C_α and C_i atoms of the benzyl ligands. Besides the Ln-C_α-C_i angles, the Ln-C_i distances are indicative for η^2-bonded benzyl groups. In the case of the above mentioned $(C_5H_5)Gd(CH_2Ph)_2(THF)$, the Gd-$C_i$ distances show values of 2.89 and 3.01 Å [26].

Based on these two criterions, it is to assume that the Nd atom in **6b** strongly interacts with the C_i atoms of all three benzyl ligands, while the Sm, Er, and Lu atoms in **7a**, **8d**, and **9d**, respectively, interact only with one of the three benzyl ligands in an η^2-fashion.

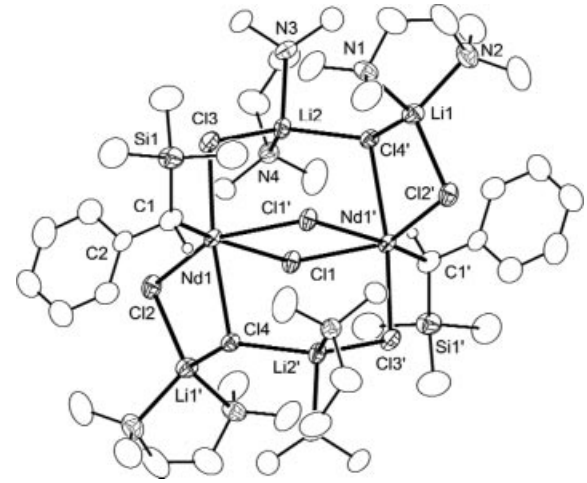

Fig. 4 Molecular structure of **10**. The hydrogen atoms except the benzyl C_α protons are omitted for clarity. Thermal ellipsoids are drawn with 30 % probability.

Selected bond lengths / Å and angles / °: Nd(1)-C(1) 2.538(7), Nd(1)-C(2) 2.876(7), Nd(1)-Cl(1) 2.7534(17), Nd(1)-Cl(1′) 2.8988(16), Nd(1)-Cl(2) 2.716(1), Nd(1)-Cl(3) 2.7219(18), Nd(1)-Cl(4) 2.8159(17), C(1)-C(2) 1.438(11); Nd(1)-C(1)-C(2) 88.1(4), C(1)-Nd(1)-C(2) 30.0(2), C(1)-C(2)-Nd(1) 61.9(4), C(1)-Nd(1)-Cl(1) 87.09(19), C(1)-Nd(1)-Cl(1′) 160.36(18), C(1)-Nd(1)-Cl(2) 101.80(19), C(1)-Nd(1)-Cl(3) 117.0(2), C(1)-Nd(1)-Cl(4) 89.11(19), C(2)-Nd(1)-Cl(1) 116.29(16), C(2)-Nd(1)-Cl(1′) 164.51(16), C(2)-Nd(1)-Cl(2) 105.09(16), C(2)-Nd(1)-Cl(3) 87.07(17), C(2)-Nd(1)-Cl(4) 85.84(16), Cl(1)-Nd(1)-Cl(1′) 74.00(5), Cl(1)-Nd(1)-Cl(2) 84.94(5), Cl(1)-Nd(1)-Cl(3) 151.66(5), Cl(1)-Nd(1)-Cl(4) 84.02(5), Cl(1′)-Nd(1)-Cl(2) 93.45(6), Cl(1′)-Nd(1)-Cl(3) 80.12(5), Cl(1′)-Nd(1)-Cl(4) 83.77(5), Cl(2)-Nd(1)-Cl(3) 95.62(6), Cl(2)-Nd(1)-Cl(4) 168.69(5), Cl(3)-Nd(1)-Cl(4) 81.85(5). Symmetry transformation used to generate equivalent atoms (′): $1-x$, $1-y$, $1-z$.

The complexes $\{[Li(tmeda)]_2[Nd(CHPhSiMe_3)Cl_4]\}_2$ (**10**) and $\{[Li(tmeda)][Nd(CHPhSiMe_3)Cl_3(THF)]\}_2$ (**11**) can be described as dimerization products of the adducts of the monobenzyl compound $Nd(CHPhSiMe_3)Cl_2$ with two (tmeda)LiCl molecules (**10**) or one (tmeda)LiCl and one THF molecule (**11**). The dimerization takes place via two chlorine bridges (Figures 4 and 5).

The center of the dimers is represented by Nd_2Cl_2 groups. The Nd(1)-Cl(1′) bonds (2.899 (**10**); 2.861 Å (**11**)) are slightly longer than the Nd(1)-Cl(1) bonds (2.753 (**10**); 2.783 Å (**11**)). The coordination polyhedron around the neodymium atoms can be described as a distorted octahedron though the angles between the axial ligands Cl(3) and Cl(4) for **10** (168.69°) and Cl(2) and O(1) for **11** (165.72°) are considerably smaller than 180°. The atoms C(1), Cl(1), Cl(1′), and Cl(2) for **10** and C(1), Cl(1), Cl(1′), and Cl(3) for **11**, respectively, are more or less in plane but are distributed unevenly around the neodymium center according to smaller Cl(1)-Nd-Cl(1′) and larger Cl(2)/(Cl(3)-Nd(1)-C(1) angles than the ideal 90° angle. This deviations are caused by the benzyl ligand which is arranged in such a way that its C(1)-C(2) bond runs almost parallel (1.5° for **10** and 5.9° for **11**) and the phenyl plane is almost perpendicular (85.7° for **10** and 74.7° for **11**) to the respective C(1)-

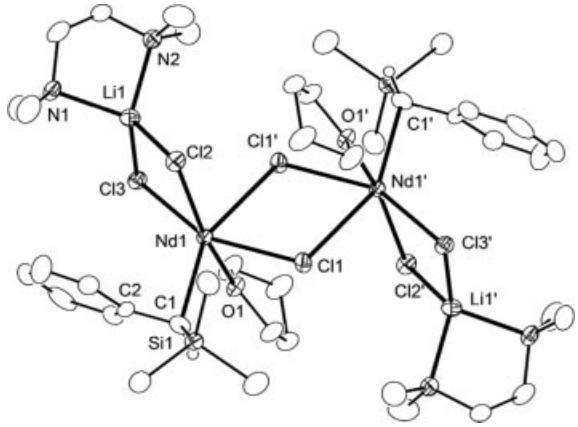

Fig. 5 Molecular structure of **11**. The hydrogen atoms except the benzyl C_α protons are omitted for clarity. Thermal ellipsoids are drawn with 30 % probability.

Selected bond lengths / Å and angles / °: Nd(1)-C(1) 2.573(9), Nd(1)-C(2) 2.777(10), Nd(1)-Cl(1) 2.783(2), Nd(1)-Cl(1′) 2.861(2), Nd(1)-Cl(2) 2.722(3), Nd(1)-Cl(3) 2.765(2), Nd(1)-O(1) 2.489(6), C(1)-C(2) 1.491(12); Nd(1)-C(1)-C(2) 81.5(6), C(1)-Nd(1)-C(2) 32.1(3), C(1)-C(2)-Nd(1) 66.4(5), C(1)-Nd(1)-Cl(1) 80.6(2), C(1)-Nd(1)-Cl(1′) 153.4(2), C(1)-Nd(1)-Cl(2) 103.9(2), C(1)-Nd(1)-Cl(3) 124.4(2), C(1)-Nd(1)-O(1) 90.3(3), C(2)-Nd(1)-Cl(1) 112.5(2), C(2)-Nd(1)-Cl(1′) 170.8(2), C(2)-Nd(1)-Cl(2) 96.1(2), C(2)-Nd(1)-Cl(3) 92.7(2), C(2)-Nd(1)-O(1) 95.0(3), Cl(1)-Nd(1)-Cl(1′) 74.42(7), Cl(1)-Nd(1)-Cl(2) 98.04(8), Cl(1)-Nd(1)-Cl(3) 154.43(7), Cl(1)-Nd(1)-O(1) 85.92(14), Cl(1′)-Nd(1)-Cl(2) 88.55(8), Cl(1′)-Nd(1)-Cl(3) 80.03(7), Cl(1′)-Nd(1)-O(1) 79.27(16), Cl(2)-Nd(1)-Cl(3) 82.32(7), Cl(2)-Nd(1)-O(1) 165.72(16), Cl(3)-Nd(1)-O(1) 88.21(14). Symmetry transformation used to generate equivalent atoms (′): $1-x$, $1-y$, $1-z$.

Cl(1)-Cl(1′)-Cl(2)/Cl(3) planes. The small Nd(1)-C(1)-C(2) (Nd-C_α-C_i) angles (88.1° (**10**); 81.5° (**11**)) together with the short Nd(1)-C(2) distances (2.88 (**10**); 2.77 Å (**11**)) point to a moderate (**10**) or even strong interaction (**11**) of the neodymium atoms with the *ipso*-carbon atom C(2) of the respective benzyl ligand.

Synthesis and Structure of $[Li(tmeda)]_2(\mu\text{-}Cl)_3Ln(CHPhSiMe_2{}^tBu)_2$

The reactions of $ErCl_3$ and $LuCl_3$ with the twofold molar amount of [Li(tmeda)][CHPhSiMe$_2$^{t}Bu] (**2**) in THF produce the μ-Cl_3 bridged compounds $[Li(tmeda)]_2(\mu\text{-}Cl)_3Ln(CHPhSiMe_2{}^tBu)_2$ (Ln = Er (**12**), Lu (**13**)) (Scheme 2)..

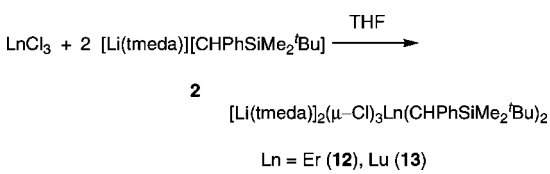

Scheme 2

Extraction of the oily residues remaining after removal of the solvent from the reaction mixtures with diethyl ether and layering the very concentrated ethereal phases with pentane, results in the formation of large pink and colorless crystals of **12** and **13**, respectively, within some days at room temperature.

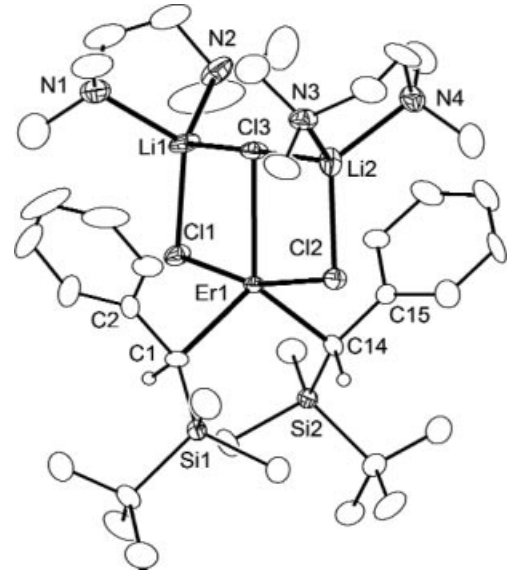

Fig. 6 Molecular structure of one of the molecules of **12**. The hydrogen atoms except the benzyl C_α protons are omitted for clarity. Only one of the two crystallographically independent molecules is shown. Thermal ellipsoids are drawn with 30 % probability.

Selected bond lengths / Å and angles / °: Er(1)-C(1) 2.368(9), Er(1)-C(2) 2.923(9), Er(1)-C(14) 2.372(9), Er(1)-C(15) 3.047(8), Er(1)-Cl(1) 2.635(2), Er(1)-Cl(2) 2.634(2), Er(1)-Cl(3) 2.703(2), C(1)-C(2) 1.492(13), C(14)-C(15) 1.487(12); Er(1)-C(1)-C(2) 95.8(5), Er(1)-C(14)-C(15) 101.8(5), C(1)-Er(1)-C(2) 30.5(3), C(14)-Er(1)-C(15) 28.5(3), C(1)-C(2)-Er(1) 53.7(4), C(14)-C(15)-Er(1) 49.6(4), C(1)-Er(1)-C(14) 109.8(3), C(1)-Er(1)-Cl(1) 94.9(2), C(1)-Er(1)-Cl(2) 95.6(2), C(1)-Er(1)-Cl(3) 125.2(5), C(14)-Er(1)-Cl(1) 94.8(2), C(14)-Er(1)-Cl(2) 92.3(2), C(14)-Er(1)-Cl(3) 125.0(2), Cl(1)-Er(1)-Cl(2) 164.54(7), Cl(1)-Er(1)-Cl(3) 82.50(7), Cl(2)-Er(1)-Cl(3) 82.18(7).

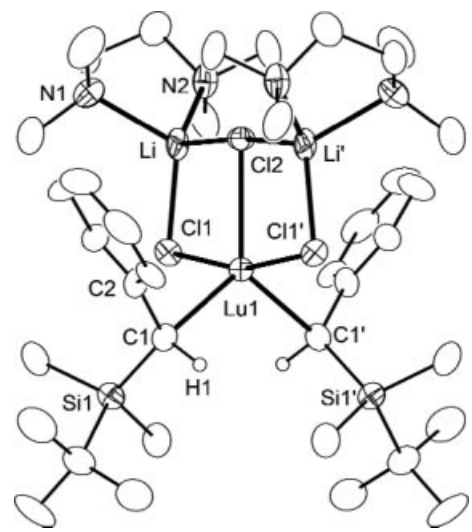

Fig. 7 Molecular structure of **13**. The hydrogen atoms except the benzyl C_α protons are omitted for clarity. Thermal ellipsoids are drawn with 30 % probability.

Selected bond lengths / Å and angles / °: Lu(1)-C(1) 2.403(7), Lu(1)-C(2) 2.918(7), Lu(1)-Cl(1) 2.5920(16), Lu(1)-Cl(2) 2.680(2), C(1)-C(2) 1.480(9); Lu(1)-C(1)-C(2) 94.5(4), C(1)-Lu(1)-C(2) 30.4(2), C(1)-C(2)-Lu(1) 55.3(2), C(1)-Lu(1)-C(1′) 109.5(3), C(1)-Lu(1)-Cl(1) 95.97(18), C(1)-Lu(1)-Cl(2) 125.26(17), C(1)-Lu(1)-Cl(1′) 93.54(17), C(1′)-Lu(1)-Cl(2) 125.26(17), C(1′)-Lu(1)-Cl(1′) 95.27(18), Cl(1)-Lu(1)-Cl(2) 82.36(4), Cl(1)-Lu(1)-Cl(1′) 164.71(8), Cl(2)-Lu(1)-Cl(1′) 82.36(4). Symmetry transformation used to generate equivalent atoms (′): x, $1.5-y$, $1.25-z$.

The crystals of **12** and **13** do not only differ with respect to the space group, but also to the crystal system. Compound **12** crystallizes monoclinic with two crystallographically independent molecules per asymmetric unit (the molecular structure of one of the molecules is depicted in Figure 6) and eight molecules per unit cell in the space group $P2_1/n$. The asymmetric unit contains both *rac*-forms. **13** exhibits a higher symmetry than **12** and crystallizes tetragonal in the space group $I\bar{4}$ 2d with eight molecules in the unit cell. Only one half of the molecule is crystallographically independent (Figure 7). The Lu(1)-Cl(2) bond lies on the C_2-axis which generates the other half of the molecule. Looking along the c-axis, the additionally fourfold rotation axis can be clearly recognized (Figure 8). Parallel to the a- and b-axes channel structures are formed (Figures 9 and 10) with pentane molecules in the cavities, originating from the crystallization process. A refinement of the solvent molecules proved to be impossible because of their disorder around the fourfold rotation axis. The solvent molecules take up a volume of 6948 Å^3 (48 %) per unit cell. The contribution of the solvent molecules was subtracted from the full data set using the SQUEZZE-routine [32] of PLATON [33].

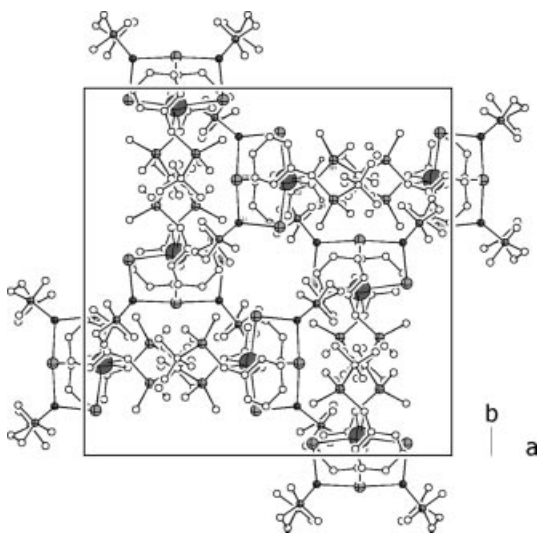

Fig. 8 Crystal packing in the structure of **13**. View along the c-axes.

The coordination polyhedron of the lanthanide atoms in these complexes resembles those in $[Li(tmeda)]_2(\mu\text{-}Cl)_3Sm(N^iPr_2)_2$ [34] or in the η^3-allenyl complex $[Li(tmeda)]_2(\mu\text{-}Cl)_3Sm[C_5H_2(SiMe_3)_2SiMe_2C_3HSiMe_3]$ [35]. The lanthanide atom is placed in the center of a distorted trigonal bipyramide formed from the C_α atoms of the two benzyl groups and the three chlorine atoms. The two C_α atoms and Cl(3) (**12**) and Cl(2) (**13**), respectively, define the equatorial plane, while the other two chlorine atoms mark the axial positions. All three chlorine atoms bridge the two [Li(tmeda)] units. The equatorial chlorine atom connects the two lithium atoms in an almost linear Li-Cl-Li fashion. The further coordination of one tmeda molecule to each

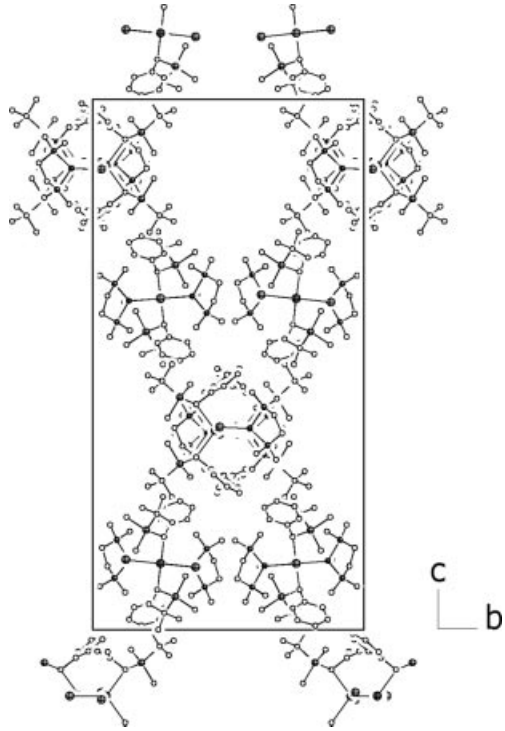

Fig. 9 Crystal packing in the structure of **13**. View along the a-axes.

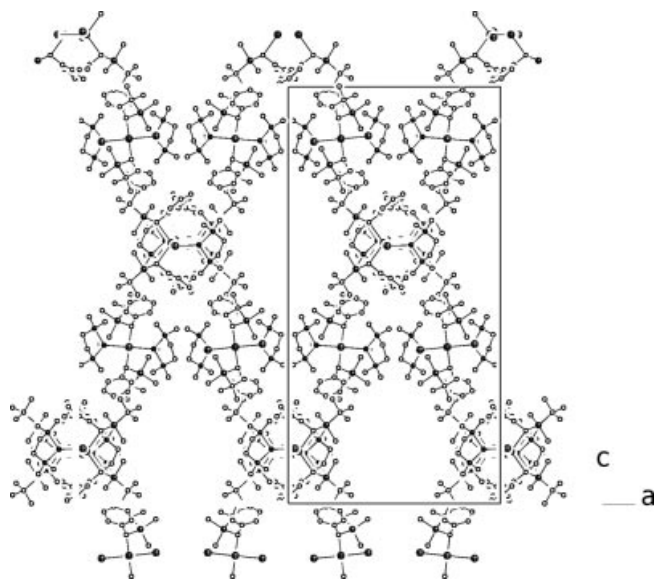

Fig. 10 Crystal packing in the structure of **13**. View along the b-axes.

lithium atom causes tetra-coordination of both lithium cations. In **12** as well as in **13**, the Ln-Cl_{ax} bond distances are shorter than the Ln-Cl_{eq} bond distance as it is the case in $[Li(tmeda)]_2(\mu\text{-}Cl)_3Sm(N^iPr_2)_2$ (Sm-Cl_{ax} 2.76 and 2.75 Å, Sm-Cl_{eq} 2.89 Å) [34], but all Ln-Cl distances in **12** and **13** are longer than those in the tris(benzyl) complexes **8d** and **9d**.

Experimental Section

General Remarks: All manipulations involving air sensitive compounds were carried out in dry, oxygen-free solvents and under an inert atmosphere of nitrogen using standard Schlenk techniques. The solvents were dried by distillation from sodium-benzophenone. Melting points were measured in sealed capillaries with a Büchi 510 melting point determination apparatus and are uncorrected. ^{1}H and ^{13}C NMR spectra were recorded on a Bruker ARX 400 (^{1}H, 400.13 MHz; ^{13}C, 100.64 MHz) spectrometer at ambient temperature. Chemical shifts are reported in ppm and referenced to the ^{1}H and ^{13}C residues of the deuterated solvents. Ln analyses were performed by complexometric titration with EDTA as indicator. Commercially available reagents were of reagent-grade quality and were used as received. [Li(tmeda)][CHPhSiMe$_3$] (**1**) [12], [Li(tmeda)][CHPhSiMe$_2$^{t}Bu] (**2**) [13], [Li(tmeda)][CHPhSiMe$_2$Ph] (**3**) [13], [Li(tmeda)][CH(C$_6$H$_3$Me$_2$-3,5)SiMe$_2$^{t}Bu] (**4**) [13], and the water-free trichlorides of Pr, Nd, Sm, Er and Lu [36] were prepared according to published procedures.

[Li(tmeda)$_2$][Pr(CHPhSiMe$_3$)$_3$Cl] (5a)

A solution of $PrCl_3$ (0.4 g, 1.62 mmol) in THF (30 mL) was treated drop wise with a solution of **1** (1.31 g, 4.57 mmol) in THF (25 mL) at room temperature. The yellow-green mixture was stirred for 12 h. Then the solvent was evaporated in vacuum and the oily residue was extracted with diethyl ether. The ethereal extract was filtered off from precipitated LiCl, then the clear solution was concentrated to 10 mL and subsequently cooled to −36 °C. In the course of 12 h light green crystals of **5a** precipitated. Yield: 0.74 g (54 %). Mp: 116−118 °C (dec). $C_{42}H_{77}ClLiN_4PrSi_3$ (905.66 g/mol): Pr 15.67 (calcd 15.56) %.

[Li(tmeda)$_2$][Pr(CHPhSiMe$_2$^{t}Bu)$_3$Cl] (5b)

5b was prepared in analogy to **5a** from $PrCl_3$ (0.35 g, 1.42 mmol) and **2** (1.49 g, 4.54 mmol). Analogous workup of the dark green to brown colored reaction mixture afforded after cooling for some days dark green crystals of **5b**. Yield: 1.31 g (89 %). Mp: 108−110 °C (dec). $C_{51}H_{95}ClLiN_4PrSi_3$ (1031.90 g/mol): Pr 14.09 (calcd 13.66) %.

[Li(tmeda)$_2$][Pr(CHPhSiMe$_2$Ph)$_3$Cl] (5c)

5c was prepared in analogy to **5a** from $PrCl_3$ (0.35 g, 1.42 mmol) and **3** (1.48 g, 4.25 mmol). Analogous workup of the dark brown-green reaction mixture and cooling for some days resulted in the precipitation of green, amorphous **5c**. Yield: 0.74 g (48 %). Mp: 110−113 °C (dec). $C_{57}H_{83}ClLiN_4PrSi_3$ (1091.87 g/mol): Pr 13.19 (calcd 12.91) %.

[Li(tmeda)$_2$][Nd(CHPhSiMe$_3$)$_3$Cl] (6a)

6a was prepared in analogy to **5a** from $NdCl_3$ (0.41 g, 1.64 mmol) and **1** (1.40 g, 4.89 mmol). Analogous workup of the orange-green reaction mixture resulted in the formation of small bunches of light green needle like crystals of **6a**. Yield: 0.47 g (31 %). Mp: 120−122 °C (dec). $C_{42}H_{77}ClLiN_4NdSi_3$ (908.99 g/mol): Nd 15.96 (calcd 15.87) %.

[Li(tmeda)$_2$][Nd(CHPhSiMe$_2$^{t}Bu)$_3$Cl] (6b)

6b was prepared in analogy to **5a** from $NdCl_3$ (0.30 g, 1.20 mmol) and **2** (1.05 g, 3.20 mmol). Analogous workup of the orange-green reaction mixture leads after standing of the concentrated ether extract at −36 °C for some weeks to the separation of small bunches of needle like crystals of **6b**. Slow cooling of a saturated ether solution of these crystals to 0 °C produces light-green single crystals of **6b**. Yield: 0.76 g (61 %). Mp: 150−155 °C (dec). $C_{51}H_{95}ClLiN_4NdSi_3$ (1035.23 g/mol): Nd 13.76 (calcd 13.93) %.

[Li(tmeda)$_2$][Sm(CHPhSiMe$_3$)$_3$Cl] (7a)

7a was prepared in analogy to **5a** from $SmCl_3$ (1.06 g, 2.65 mmol) and **1** (2.20 g, 7.68 mmol). Analogous workup of the dark violet reaction mixture resulted in the formation of small, dark violet crystals of **7a**. Slow cooling of a saturated ethereal solution of these crystals to −36 °C yielded rectangular single crystals. Yield: 0.75 g (31 %). Mp: 139−140 °C (dec). $C_{42}H_{77}ClLiN_4Si_3Sm$ (915.11 g/mol): Sm 16.82 (calcd 16.43) %.

^{1}H NMR (400 MHz, pyridine-d$_5$): δ = −0.2 to −1.6 (m, 27H, SiMe$_3$), 1.8−2.1 (m, 3H, CH), 2.17 (s, 24H, NCH$_3$), 2.39 (s, 8H, NCH$_2$), 7.0−7.5 (m, 15H, Ph).

[Li(tmeda)$_2$][Sm(CHPhSiMe$_2$^{t}Bu)$_3$Cl] (7b)

7b was prepared in analogy to **5a** from $SmCl_3(THF)_2$ (0.37 g, 0.93 mmol) and **2** (0.89 g, 2.71 mmol). Analogous workup of the violet reaction mixture and cooling for 2 d afforded small bunches of dark violet, needle like crystals of **7b**. Slow cooling of a saturated solution of these crystals in toluene first to 0 °C and then to −36 °C led to the formation of almost black crystals of the mono toluene adduct of **7b**. Yield: 0.50 g (53 %). Mp: 142−144 °C (dec). $C_{51}H_{95}ClLiN_4Si_3Sm$ (1041.35 g/mol): Sm 14.98 (calcd 14.44) %.

^{1}H NMR (400 MHz, pyridine-d_5): δ = −0.09 (s, 9H, SiCH$_3$), 0.14 (s, 9H, SiCH$_3$), 0.35 (s, 27H, ^{t}Bu), 2.11 (s, 3H, CH), 2.17 (s, 24H, NCH$_3$), 2.38 (s, 8H, NCH$_2$), 6.92−7.44 (m, 15H, Ph).

[Li(tmeda)$_2$][Er{CH(C$_6$H$_3$Me$_2$-3,5)SiMe$_2$^{t}Bu}$_3$Cl] (8d)

8d was prepared in analogy to **5a** from $ErCl_3$ (0.41 g, 1.5 mmol) and **4** (1.56 g, 4.37 mmol). Analogous workup of the orange-pink reaction mixture resulted in the formation of light pink crystals of **8d**. Slow cooling of a saturated ethereal solution of this crystals to −36 °C afforded square pink single crystals of **8d**(Et_2O)$_2$. Drying of the adduct in vacuum gave ether free **8d**. Yield: 0.68 g (40 %). Mp: 152−153 °C (dec). $C_{57}H_{107}ClErLiN_4Si_3$ (1142.41 g/mol): Er 14.33 (calcd 14.64) %.

[Li(tmeda)$_2$][Lu{CH(C$_6$H$_3$Me$_2$-3,5)SiMe$_2$^{t}Bu)$_3$Cl] (9d)

9d was prepared in analogy to **5a** from $LuCl_3(THF)_3$ (0.71 g, 1.41 mmol) and **4** (1.56 g, 4.35 mmol). Analogous workup of the light yellow reaction mixture resulted in the formation of colorless microcrystalline **9d**. Slow cooling of a saturated ethereal solution of these crystals to −36 °C produced big square crystals of **9d**(Et_2O). Drying of the adduct in vacuum gave ether free **9d**. Yield: 0.86 g (53 %). Mp: 120−122 °C. $C_{57}H_{107}ClLiLuN_4Si_3$ (1150.12 g/mol)): Lu 15.31 (calcd 15.21) %.

^{1}H NMR (400 MHz, pyridine-d_5): δ = 0.08 (s, 9H, SiCH$_3$), 0.28 (s, 9H, SiCH$_3$), 0.60 (s, 27H, C(CH$_3$)$_3$), 2.07 (s, 8H, C*H*$_3$C$_6$H$_3$), 2.15 (s, 10H,

$CH_3C_6H_3$), 2.16 (s, 24H, NCH_3), 2.20 (s, 3H, LuCH), 2.32 (s, 8H, NCH_2), 5.60 (s, 3H, C_6H_3), 6.18 (s, 3H, C_6H_3), 6.56 (s, 3H, C_6H_3). **$^{13}C\{^1H\}$ NMR** (100.64 MHz, THF-d_8): δ = −1.9 ($SiCH_3$), −1.5 ($SiCH_3$), 21.9 ($CH_3C_6H_3$), 27.0 ($C(CH_3)_3$), 28.5 ($C(CH_3)_3$), 46.3 (NCH_3), 58.8 (NCH_2), 61.2 (LuCH), 125.7, 126.2 (C^p), 136.9, 138.0 (C^o/C^m), 151.7 (C^{ipso}).

{[Li(tmeda)]$_2$[Nd(CHPhSiMe$_3$)Cl$_4$]}$_2$ (10) and {[Li(tmeda)][Nd(CHPhSiMe$_3$)Cl$_3$(THF)]}$_2$ (11)

10 and **11** were prepared in analogy to **5a** from $NdCl_3$ (0.63 g, 2.51 mmol) and **1** (2.16 g, 7.54 mmol). After layering the very concentrated ethereal solution (4 mL) with pentane (8 mL) at room temperature, light green crystals of **10** separated within 12 h and after further 24 h orange crystals of **11** precipitated. Single crystals of both kinds were separated from the crystal mixture with the help of a microscope. They were characterized by X-ray structure analysis. Yield: 1.68 g.

[Li(tmeda)]$_2$(μ-Cl)$_3$Er(CHPhSiMe$_2$^{t}Bu)$_2$ (12)

12 was prepared in analogy to **5a** from $ErCl_3$ (0.33 g, 1.21 mmol) and **2** (0.77 g, 2.34 mmol). After analogous workup of the yellow-pink reaction mixture, the concentrated ethereal solution (4 mL) was covered with a layer of pentane (8 mL) at room temperature. Big pink crystals of **12** separated after 2 weeks. Yield: 0.64 g (59 %). Mp: 120 °C (dec.). $C_{38}H_{74}Cl_3ErLi_2N_4Si_2$ (930.70 g/mol): Er 18.08 (calcd 17.97) %.

[Li(tmeda)]$_2$(μ-Cl)$_3$Lu(CHPhSiMe$_2$^{t}Bu)$_2$ (13)

13 was prepared in analogy to **5a** from $LuCl_3$ (0.57 g, 2.03 mmol) and **2** (1.32 g, 4.02 mmol). After analogous workup of the light yellow reaction mixture and cooling of the ethereal phase to −78 °C, a colorless microcrystalline precipitate formed. Covering of a concentrated ethereal solution of this precipitate (4 mL) with pentane (8 mL) at room temperature produced colorless crystals of **13** within a few days. Yield: 0.79 g (41 %). Mp: 100 °C (dec.). $C_{57}H_{107}ClLiLuN_4Si_3$ (1150.12 g/mol): Lu 15.31 (calcd 15.21) %.

^1H NMR (400 MHz, pyridine-d_5): δ = −0.12 to −0.03 (m, 6H, $SiCH_3$), 0.18−0.34 (m, 6H, $SiCH_3$), 0.73−0.85 (m, 18H, $C(CH_3)_3$), 2.167 (d, 24H, NCH_3), 2.37 (d, 8H, NCH_2), 2.55, 2.56 (2H, LuCH), 7.06−7.48 (m, 10H, Ph). **$^{13}C\{^1H\}$ NMR** (100.64 MHz, pyridine-d_5): δ = −4.8 ($SiCH_3$), −4.6 ($SiCH_3$), 17.7 ($C(CH_3)_3$), 27.1 ($C(CH_3)_3$), 45.5 (NCH_3), 47.4, 47.5 (LuCH), 57.7 (NCH_2), 123.7, 124.0 (C^p), 127.4, 128.2, 128.3, 130.7, 130.8 (C^o/C^m), 145.5 (C^{ipso}).

X-Ray structure determination

Crystal data and refinement parameters are listed in Tables 2 and 3. The data were collected on a Siemens SMART CCD diffractometer (graphite-monochromated Mo Kα radiation, λ = 0.71073 Å) by use of ω scans at 173 K. The structures were solved by direct methods and were refined on F^2 using all reflections with the SHELX-97 software package [37]. Most non-hydrogen atoms were refined anisotropically. Most hydrogen atoms were placed in calculated positions and assigned to an isotropic displacement parameter of 0.08 Å^2. In **7a** all atoms and in **8d/9d** all carbon atoms of one tmeda ligand are disordered about two positions (occupancy factors **7a**: 0.347(13)/0.653(13); **8d**: 0.383(11)/0.617(11); **9d**: 0.49(3)/0.51(3)). Additionally, one diethyl ether molecule in **8d/9d** was found to be disordered about two positions (occupancy factors **8d**: 0.579(10)/0.617(11); **9d**: 0.47(3)/0.53(3)). These atoms were refined isotropically. SADABS was used to perform area-detector scaling and absorption corrections for **6b**, **7a**, **8d**, **9d**, **10**, **11**, and **12** [38]. CCDC-685203 (**6b**), CCDC-685204 (**7a**), CCDC-685205 (**8d**), CCDC-685206 (**9d**), CCDC-685207 (**10**), CCDC-685208 (**11**), CCDC-685209 (**12**), and CCDC-685210 (**13**) contain the supplementary crystallographic data. These data can be obtained free of charge at www.ccdc.cam.ac.uk/conts/retrieving.html [or from the

Table 2 Crystal data and structure refinement parameters for **6b**, **7a**, **8d**, **9d**, and **10**.

Compound	**6b**	**7a**	**8d**	**9d**	**10**
Chemical formula	$C_{51}H_{95}ClLiN_4NdSi_3$	$C_{42}H_{77}ClLiN_4Si_3Sm$	$C_{65}H_{126}ClErLiN_4O_2Si_3$	$C_{65}H_{126}ClLiLuN_4O_2Si_3$	$C_{44}H_{94}Cl_8Li_4N_8Nd_2Si_2$
Formula weight	1035.21	915.09	1289.62	1297.33	1391.32
Crystal size/mm^3	0.45×0.24×0.12	0.52×0.18×0.12	0.44×0.24×0.20	0.78×0.55×0.30	0.44×0.30×0.12
Crystal system	triclinic	monoclinic	monoclinic	monoclinic	triclinic
Space group	$P\bar{1}$ (No. 2)	$P2_1/n$ (No. 14)	$P2_1/c$ (No. 14)	$P2_1/c$ (No. 14)	$P\bar{1}$ (No. 2)
a/Å	13.3015(2)	17.4502(3)	12.6862(2)	12.6549(2)	11.4973(3)
b/Å	15.0814(2)	14.5461(2)	25.1686(3)	25.2826(3)	12.8026(4)
c/Å	16.4227(2)	21.1495(1)	24.3523(2)	24.4188(3)	13.1068(4)
α/°	83.858(1)				91.502(1)
β/°	89.359(1)	109.517(1)	99.748(1)	99.650(1)	97.324(1)
γ/°	65.581(1)				116.289(1)
V/Å^3	2980.57(7)	5059.97(11)	7663.28(16)	7702.21(18)	1708.17(9)
Z	2	4	4	4	1
ρ_{calcd} /(g/cm^3)	1.15	1.20	1.12	1.12	1.35
F(000)	1102	1924	2760	2772	710
μ (Mo K$_\alpha$)/mm^{-1}	1.009	1.314	1.215	1.401	1.884
Max. / min. trans.	0.9138 / 0.6156	0.8898 / 0.6016	0.8898 / 0.6015	0.6999 / 0.4654	0.8463 / 0.4419
Index ranges	$-15 \le h \le 16$	$-20 \le h \le 16$	$-13 \le h \le 16$	$-15 \le h \le 15$	$-13 \le h \le 14$
	$-18 \le k \le 18$	$-13 \le k \le 17$	$-25 \le k \le 32$	$-30 \le k \le 29$	$-16 \le k \le 16$
	$-20 \le l \le 20$	$-25 \le l \le 25$	$-31 \le l \le 23$	$-29 \le l \le 23$	$-16 \le l \le 17$
θ-range /°	1.25 − 26.00	1.32 − 25.00	1.17 − 27.50	1.17 − 25.00	1.57 − 27.50
Measured refl.	20185	30413	46733	46204	13114
Unique refl. [R_{int}]	11605 [0.0962]	8910 [0.1152]	17271 [0.0952]	13451 [0.1464]	7733 [0.0894]
Param. / restraints	585 / 0	492 / 0	697 / 48	697 / 48	322 / 0
GOF on F^2	0.891	0.966	1.011	1.159	0.902
R_1 [$I>2\sigma(I)$]	0.0636	0.0498	0.0591	0.1019	0.0592
wR_2 (all data)	0.1182	0.0893	0.1228	0.2363	0.1240
Larg. Diff. peak and hole /(e/Å^3)	0.956 / −1.349	0.593 / −0.964	1.159 / −0.753	2.386 / −1.429	1.171 / −1.019

Table 3 Crystal data and structure refinement parameters for **11**, **12**, and **13**.

Compound	**11**	**12**	**13**
Chemical formula	$C_{40}H_{78}Cl_6Li_2N_4Nd_2O_2Si_2$	$C_{38}H_{74}Cl_3ErLi_2N_4Si_2$	$C_{38}H_{74}Cl_3Li_2LuN_4Si_2$
Formula weight	1218.30	930.68	938.39
Crystal size/mm^3	0.30×0.26×0.10	0.44×0.35×0.30	0.76×0.48×0.42
Crystal system	triclinic	monoclinic	tetragonal
Space group	$P\bar{1}$ (No. 2)	$P2_1/n$ (No. 14)	$I\bar{4}2d$ (No. 122)
a/Å	11.3611(3)	19.1949(2)	19.9294(3)
b/Å	11.6332(2)	25.2650(2)	19.9294(3)
c/Å	11.9492(3)	21.2555(2)	39.0981(9)
α/°	85.463(1)		
β/°	74.199(1)	100.789(1)	
γ/°	68.712(1)		
V/Å^3	1415.57(6)	10125.83(16)	15529.0(5)
Z	1	8	8
ρ_{calcd} /(g/cm^3)	1.43	1.22	0.80
$F(000)$	618	3864	3888
μ (Mo K_α)/mm^{-1}	2.172	1.890	1.423
Max. / min. trans.	0.8516 / 0.4254	0.6630 / 0.2788	–
Index ranges	$-14 \le h \le 8$	$-23 \le h \le 23$	$-21 \le h \le 22$
	$-15 \le k \le 14$	$-31 \le k \le 25$	$-22 \le k \le 22$
	$-15 \le l \le 15$	$-24 \le l \le 26$	$-40 \le l \le 44$
θ-range /°	1.17 – 27.50	1.27 – 26.00	1.15 – 24.00
Measured refl.	10802	55984	42373
Unique refl. [R_{int}]	6430 [0.0996]	19814 [0.1169]	6074 [0.1613]
Param. / restraints	269 / 0	952 / 0	240 / 0
GOF on F^2	0.978	1.012	1.007
R_1 [$I>2\sigma(I)$]	0.0714	0.0712	0.0542
wR_2 (all data)	0.1432	0.1781	0.0969
Larg. Diff. peak and hole /(e/Å^3)	1.790 / −2.113	2.102 / −3.916	0.960 / −0.601

Cambridge Crystallographic Data Centre, 12, Union Road, Cambridge CB2 1EZ, UK»x: (internat.) +44-1223/336-033; E-mail: deposit@ccdc.cam.ac.uk].

Acknowledgements. This work was supported by the Fonds der Chemischen Industrie and the Deutsche Forschungsgemeinschaft (SPP "Lanthanoidspezifische Funktionalitäten in Molekül und Material").

References

[1] Part 182: H. Schumann, M. Hummert, A. N. Lukoyanov, V. A. Chudakova, I. L. Fedushkin, *Z. Naturforsch.* **2007**, *62b*, 1–5.

[2] a) F. T. Edelmann, *Angew. Chem.* **1995**, *107*, 2647–2669; *Angew. Chem. Int. Ed. Engl.* **1995**, *34*, 2466–2488; b) F. T. Edelmann, D. M. M. Freckmann, H. Schumann, *Chem. Rev.* **2002**, *102*, 1851–1896; v) W. E. Piers, D. J. H. Emslie, *Coord. Chem. Rev.* **2002**, *233–234*, 131–155.

[3] L. E. Manzer, *J. Am. Chem. Soc.* **1978**, *100*, 8068–8073.

[4] a) I. S. Guzman, N. N. Chigir, O. K. Sharaev, G. N. Bondarenko, E. I. Tinyakova, B. A. Dolgoplosk, *Dokl. Akad. Nauk SSSR* **1979**, *249*, 860–862; *Proc. Acad. Sci. USSR* **1979**, *249*, 519–521; b) B. A. Dolgoplosk, E. I. Tinyakova, I. S. Guzman, E. L. Vollerstein, N. N. Chigir, G. N. Bondareno, O. K. Sharaev, V. A. Yakovlev, *J. Organomet. Chem.* **1980**, *201*, 249–255; c) N. N. Chigir, I. S. Guzman, O. K. Sharaev, E. I. Tinyakova, B. A. Dolgoplosk, *Dokl. Akad. Nauk SSSR* **1982**, *263*, 375–378; *Proc. Acad. Sci. USSR* **1982**, *263*, 105–108.

[5] K. H. Thiele, K. Unverhau, M. Geitner, K. Jacob, *Z. Anorg. Allg. Chem.* **1987**, *548*, 175–179.

[6] A. Mandel, J. Magull, *Z. Anorg. Allg. Chem.* **1997**, *623*, 1542–1546.

[7] S. Harder, *Organometallics* **2005**, *24*, 373–379.

[8] S. Bambirra, A. Meetsma, B. Hessen, *Organometallics* **2006**, *25*, 3454–3462.

[9] N. Meyer, P. W. Roesky, S. Bambirra, A. Meetsma, B. Hessen, K. Saliu, J. Takats, *Organometallics* **2008**, *27*, 1501–1505.

[10] S. Harder, C. Ruspic, N. N. Bhriain, F. Berkermann, M. Schürmann, *Z. Naturforsch.* **2008**, *63b*, 267–274.

[11] H. Schumann, D. M. M. Freckmann, S. Dechert, *Organometallics* **2006**, *25*, 2696–2699.

[12] L. Brandsma, *Preparative Polar Organometallic Chemistry*, Vol. 2, Springer Verlag: Berlin, 1990.

[13] H. Schumann, D. M. M. Freckmann, S. Dechert, *Z. Anorg. Allg. Chem.*, **2008**, *634*, 1334–1338.

[14] J. L. Atwood, W. E. Hunter, R. D. Rogers, J. Holton, J. McMeeking, R. Pearce, M. F. Lappert, *J.Chem. Soc. Chem.Commun.* **1978**, 140–142.

[15] F. T. Edelmann, A. Steiner, D. Stalke, J. W. Gilje, S. Jagner, M. Hakansson, *Polyhedron* **1994**, *13*, 539–546.

[16] J. L. Atwood, M. F. Lappert, R. G. Smith. H. Zhang, *J. Chem. Soc. Chem. Commun.* **1988**, 1308–1309.

[17] P. B. Hitchcock, M. F. Lappert, R. G. Smith, *J. Chem. Soc. Chem. Commun.* **1989**, 369–371.

[18] O. Just, W. S. Rees, *Inorg. Chem.* **2001**, *40*, 1751–1755.

[19] H. Schumann, J. Winterfeld, E. C. E. Rosenthal, H. Hemling, L. Esser, *Z. Anorg. Allg. Chem.* **1995**, *621*, 122–130.

[20] H. Schumann, F. Erbstein, J. Demtschuk, R. Weimann, *Z. Anorg. Allg. Chem.* **1999**, *625*, 1457–1465.

[21] J. S. Xia, Z. S. Jin, W. Q. Chen, *Chin. J. Chem.* **1996**, *13*, 31–39.

[22] H. Schumann, F. Erbstein, D. Karasiak, I. L. Fedushkin, J. Demtschuk, F. Girgsdies, *Z. Anorg. Allg. Chem.* **1999**, *625*, 781–788.

[23] R. D. Shannon, *Acta Cryst. A* **1976**, *32*, 751–767.

[24] H. Schumann, D. M. M. Freckmann, S. Dechert, *Z. Anorg. Allg. Chem.* **2992**, *628*, 2422−2426.
[25] M. Booij, A. Meetsma, J. H. Teuben, *Organometallics* **1991**, *10*, 3246−3252.
[26] A. Mandel, J. Magull, *Z. Anorg. Allg. Chem.* **1996**, *622*, 1913−1919.
[27] W. J. Evans, T. A. Ulibarri, J. W. Ziller, *Organometallics* **1991**, *10*, 134−142.
[28] S. Bambirra, M. J. R. Brandsma, E. A. C. Brussee, A. Meetsma, B. Hessen, J. H. Teuben, *Organometallics* **2000**, *19*, 3197−3204.
[29] (a) R. F. Jordan, R. E. LaPointe, N. Baenzinger, G. D. Hich, *Organometallics* **1990**, *9*, 1539−1545; (b) C. Pellecchia, A. Grassi, A. Immirzi, *J. Am. Chem. Soc.* **1993**, *115*, 1160−1162; (c) C. Pellecchia, A. Immirzi, D. Pappalardo, A. Peluso, *Organometallics* **1994**, *13*, 3773−3775.
[30] E. A. Mintz, K. G. Moloy, T. J. Marks, V. W. Day, *J. Am. Chem. Soc.* **1982**, *104*, 4692−4695.
[31] P. G. Edwards, R. A. Andersen, A. Zalkin, *Organometallics* **1984**, *3*, 293−298.
[32] P. van der Sluis, A. L. Spek, *Acta Cryst.* **1990**, *A46*, 194−201.
[33] A. L. Spek, PLATON A Multipurpose Crystallographic Tool, Utrecht University **2000**.
[34] R. K. Minhas, Y. Ma, J. I. Song, S. Gambarotta, *Inorg. Chem.* **1996**, *35*, 1866−1873.
[35] E. Ihara, M. Tanaka, H. Yasuda, N. Kanehisa, T. Maruo, Y. Kai, *J. Organomet. Chem.* **2000**, *613*, 26−32.
[36] G. Brauer, Handbuch der präparativen Anorganischen Chemie, F. Enke Verlag, Stuttgart (1962).
[37] (a) G. M. Sheldrick, *SHELXL-97 Program for Crystal Structure Refinement*, Universität Göttingen (Germany) **1997**; (b) G. M. Sheldrick, *SHELXS-97 Program for Crystal Structure Solution*, Universität Göttingen (Germany) **1997**.
[38] G. M. Sheldrick, *SADABS, Program for Empirical Absorption Correction of Area Detector Data*, Universität Göttingen (Germany) **1996**.

